JOURNAL OF THE ROYAL SOCIETY Interface

J. R. Soc. Interface (2010) **7**, 1723–1733
doi:10.1098/rsif.2010.0207
Published online 2 June 2010

Biomechanical properties of single chondrocytes and chondrons determined by micromanipulation and finite-element modelling

Bac V. Nguyen[1], Qi Guang Wang[2], Nicola J. Kuiper[2], Alicia J. El Haj[2], Colin R. Thomas[1] and Zhibing Zhang[1,*]

[1]*School of Chemical Engineering, University of Birmingham, Edgbaston, Birmingham B15 2TT, UK*
[2]*Institute for Science and Technology in Medicine, University of Keele, Staffordshire ST5 5BG, UK*

A chondrocyte and its surrounding pericellular matrix (PCM) are defined as a chondron. Single chondrocytes and chondrons isolated from bovine articular cartilage were compressed by micromanipulation between two parallel surfaces in order to investigate their biomechanical properties and to discover the mechanical significance of the PCM. The force imposed on the cells was measured directly during compression to various deformations and then holding. When the nominal strain at the end of compression was 50 per cent, force relaxation showed that the cells were viscoelastic, but this viscoelasticity was generally insignificant when the nominal strain was 30 per cent or lower. The viscoelastic behaviour might be due to the mechanical response of the cell cytoskeleton and/or nucleus at higher deformations. A finite-element analysis was applied to simulate the experimental force-displacement/time data and to obtain mechanical property parameters of the chondrocytes and chondrons. Because of the large strains in the cells, a nonlinear elastic model was used for simulations of compression to 30 per cent nominal strain and a nonlinear viscoelastic model for 50 per cent. The elastic model yielded a Young's modulus of 14 ± 1 kPa (mean $\pm$ s.e.) for chondrocytes and 19 ± 2 kPa for chondrons, respectively. The viscoelastic model generated an instantaneous elastic modulus of 21 ± 3 and 27 ± 4 kPa, a long-term modulus of 9.3 ± 0.8 and 12 ± 1 kPa and an apparent viscosity of 2.8 ± 0.5 and 3.4 ± 0.6 kPa s for chondrocytes and chondrons, respectively. It was concluded that chondrons were generally stiffer and showed less viscoelastic behaviour than chondrocytes, and that the PCM significantly influenced the mechanical properties of the cells.

Keywords: chondrocyte; chondron; finite-element modelling; micromanipulation; nonlinear elasticity; viscoelasticity

1. INTRODUCTION

Articular cartilage is composed of chondrocytes, collagens, proteoglycans, hyaluronan and other non-collagenous proteins, which are organized into a highly hydrated and structured extracellular matrix with unique biological and mechanical properties (Buckwalter & Mankin 1998). Chondrocytes produce a hydrated pericellular matrix (PCM); together they form 'chondrons' (Szirmai 1974). The PCM plays an important role in transferring mechanical signals between chondrocytes and their surrounding extracellular matrix. The precise function of the PCM is not known but it clearly has a major impact in regulating the biomechanical environment of the chondrocytes, as well as influencing their activity (Poole 1997). Understanding the mechanical properties of chondrocytes and chondrons and how the PCM influences the cell response to mechanical stimuli will be vital to engineering functional cartilage and the aim of this study was to explore these issues in detail.

The biomechanical properties of chondrocytes and chondrons have been investigated using various experimental techniques including deformation within an agarose gel (Lee *et al.* 2000), micropipette aspiration (Trickey *et al.* 2000), atomic force microscopy (Allen & Mao 2004), cytoindentation and cytodetachment (Athanasiou *et al.* 1999; Koay *et al.* 2003) and modified cytoindentation, also called unconfined creep compression (Leipzig & Athanasiou 2005; Shieh & Athanasiou 2006), in conjunction with theoretical models. Most of these techniques required cells to be anchorage-dependent (Ofek & Athanasiou 2007), while micropipette aspiration and AFM in conjunction

*Author for correspondence (z.zhang@bham.ac.uk).

Received 8 April 2010
Accepted 11 May 2010

with custom-made pyramidal wells have been applied to single cells in suspension. Since the cells in cartilage may experience large compression deformation under applied joint pressure (Wong & Carter 2003), it is crucial to understand the mechanical properties of single cells under large deformation. Among the techniques mentioned above, only modified cytoindentation can generate direct and large deformation of the cells (in creep tests). However, it requires seeding the chondrocyte onto a substrate, which can modify its phenotype. The maintenance of phenotype, particularly cell shape, is important when assessing the mechanical response of cells (Guilak *et al.* 1997).

Because of these problems and the use of different tissue sources, published data on chondrocyte elastic modulus differ by two orders of magnitude, with reported values in the range 0.1–8 kPa (Trickey *et al.* 2000; Koay *et al.* 2003; Shieh & Athanasiou 2006). Chondrons have received less attention than chondrocytes since their isolation procedure involves slow-speed serial homogenization that gives a very low yield (1–2%) of viable, reproducible chondron preparations (Poole *et al.* 1988). Also, chondron preparations cannot be separated from the associated tissue and collagenous debris. Enzymatically prepared chondron techniques provide a higher cell yield, a better cell viability and preparations that are free from tissue debris (Lee *et al.* 1997). The mechanical properties of single chondrons have been investigated by micropipette aspiration (Alexopoulos *et al.* 2003; Guilak *et al.* 2005) and AFM (Ng *et al.* 2007). These techniques are powerful in determining local mechanical properties of the PCM since they only deform a portion of the PCM and cannot be used to apply forces or controlled deformations on a whole single chondron. Reported values of the elastic modulus of the PCM also show significant variations from 1.5 to *ca* 70 kPa depending on the osteoarthritic and zonal differences of the cells (Guilak *et al.* 1999; Alexopoulos *et al.* 2003; Ofek & Athanasiou 2007).

Measurement of the forces corresponding to large deformations including bursting may be realized by directly compressing single chondrocytes and chondrons in suspension using micromanipulation (Nguyen *et al.* 2009*b*). This also enables tests of both compression–holding and compression–release. Using this technique, the force imposed on the chondrocytes and chondrons has been measured directly during compression to different deformations at various speeds. It was found that elastic behaviour was dominant when the nominal strain was 30 per cent or less while there was considerable viscoelasticity when the nominal strain was 50 per cent or more, indicating strain-dependent or nonlinear viscoelastic behaviour (Nguyen *et al.* 2009*b*). Deformations such as these are found *in vivo* (Wong & Carter 2003) and are typical of those used for studies of mechanical stimulation (Caille *et al.* 2002; Koay *et al.* 2008; Leipzig & Athanasiou 2008). For example, the superficial zone in articular cartilage can experience compressive strains in the range of 60 per cent (Wong & Carter 2003).

To extract the biomechanical properties of cells, experimental compression data must be mathematically modelled using an appropriate constitutive model for the cell material. Both elastic and viscoelastic models have been used extensively for simulation of cells under compression (Trickey *et al.* 2000; Guilak *et al.* 2002; Koay *et al.* 2003; Leipzig & Athanasiou 2005; Shieh & Athanasiou 2006) and a more complex linear biphasic model has been applied to chondrocyte–PCM interactions (Guilak & Mow 2000; Lee *et al.* in press). In these elastic and viscoelastic models, the cell was assumed to be an isotropic, homogeneous, linear elastic or viscoelastic solid, and in most cases, it was assumed that the material of the cell is incompressible. Of course, cells are actually highly heterogeneous and anisotropic, with intracellular components (cytoskeleton, nucleus, cytoplasm and several other organelles). Nevertheless, these assumptions make it possible to characterize cell mechanical properties easily and to understand how the properties vary under different conditions. It was also generally assumed that the strain generated during compression is small so that linear elastic or viscoelastic models could be applied. However, if a cell is compressed to large cell deformations (Shieh *et al.* 2006; Koay *et al.* 2008; Nguyen *et al.* 2009*b*), large strains (e.g. 5% or more) might be generated and nonlinear elastic or viscoelastic models should then be preferable. In this case, suitable constitutive equations might be obtained by assuming that the cell is hyperelastic, in which case the stress components can be derived from an appropriate strain energy function. While there are many types of strain energy function that might be chosen for modelling, the neo-Hookean material model (Rivlin 1948) has been used successfully to describe nonlinear elastic behaviour of cells in compression experiments on endothelial cells (Caille *et al.* 2002) and eukaryotic cells (Peeters *et al.* 2005), and in the absence of better information, the neo-Hookean model was applied to chondrocytes and chondrons in this work. However, chondrocytes and chondrons were found to be viscoelastic at large deformations, and showed significant force relaxation after compression (Nguyen *et al.* 2009*b*). Therefore, a nonlinear viscoelastic model had to be developed to describe their behaviour at such deformations.

In this paper, experimental data of single chondrocytes and chondrons from compression–holding and compression–release experiments (Nguyen *et al.* 2009*b*) were interpreted using finite-element simulations. An incompressible, isotropic, homogeneous, neo-Hookean nonlinear elastic model was used for modelling their compressions up to 30 per cent nominal strain, while an equivalent nonlinear but viscoelastic material model was used for modelling compressions up to 50 per cent nominal strain. Intrinsic biomechanical property parameters of the chondrocytes and chondrons as single cells (assumed to be homogeneous) were then determined.

2. MATERIAL AND METHODS

2.1. Materials and cell preparation

Chondrocytes and chondrons were isolated enzymatically from full-depth articular cartilage that had been dissected from the trochleal humerus of 18-month-old

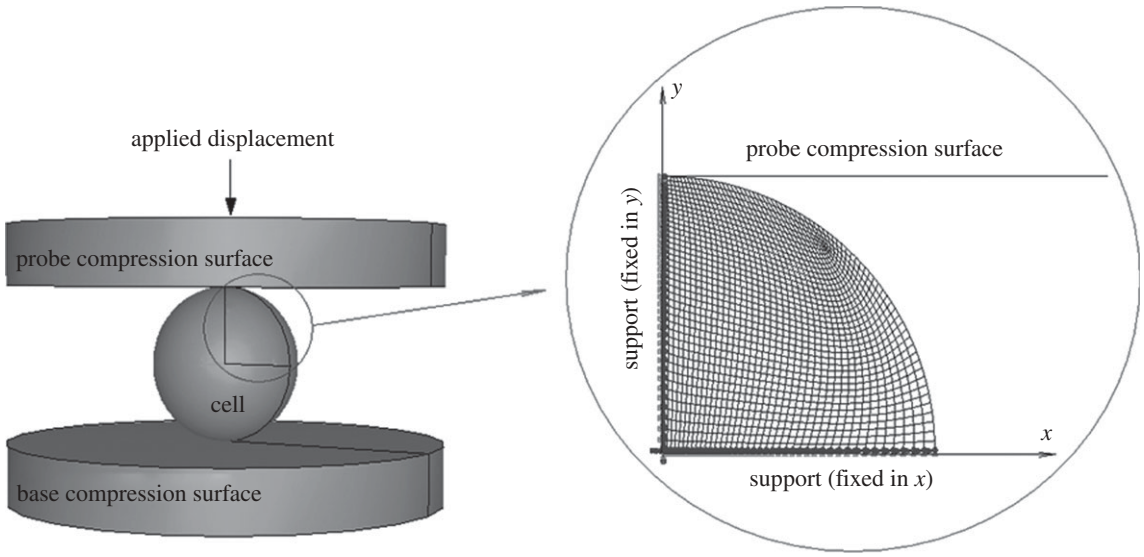

Figure 1. A three-dimensional schematic of the compression experiment and its finite-element mesh and boundary conditions.

cows as described by Wang *et al.* (2008, 2009, 2010). Four separate isolations were undertaken, each using one humerus. Isolation of chondrocytes was performed as described previously (Kuettner *et al.* 1982; Wang *et al.* 2008). Briefly, diced cartilage was sequentially digested with 700 U ml^{-1} Pronase E (Gibco) for 1 h, then 200 U ml^{-1} collagenase XI (Sigma) and 0.1 mg ml^{-1} DNase I (Sigma) for 16 h. Chondrocytes from the supernatant were separated through a 70 μm cell sieve, washed in Dulbecco's Modified Eagle's Medium (DMEM, Gibco) supplemented with 10% (v/v) foetal calf serum (FCS, Gibco) and centrifuged at 750 *g*. The cells were washed three times.

For isolation of chondrons, a previously published protocol (Lee *et al.* 1997) was modified. Again, four separate isolations were carried out, each using one humerus. Diced cartilage was digested with 3.3 U ml^{-1} dispase (Gibco) and 560 U ml^{-1} collagenase type XI (Sigma) in DMEM for 5 h. These conditions achieved the optimal cell viability and cell yield (data not shown). The cell suspension was filtered through a 70-μm cell sieve, washed in DMEM supplemented with 10 per cent FCS and centrifuged at 400 *g*. The cells were washed three times.

Both the isolated chondrocytes and chondrons were fully characterized using a number of techniques including immunohistochemistry (Wang *et al.* 2008). Using immunohistochemistry, typical PCM markers were present around the chondrons but not the chondrocytes These previously published data (Wang *et al.* 2008) demonstrated the efficacy of the enzymatic isolation procedure. The chondrocytes and chondrons remained viable (greater than 94%) for greater than 10 h as assessed by Trypan Blue (Sigma) exclusion and Live/Dead Cell Staining (Sigma).

Mechanical tests on cells were started immediately after isolation and were carried out within 9 h. The experiments were conducted at room temperature of 22 ± 1°C. To maintain good viability and hydration, all cells were kept in DMEM supplemented with 10 per cent FCS throughout the whole testing period.

2.2. Micromanipulation testing

The principle of the micromanipulation technique is to compress single chondrocytes or chondrons, suspended in culture medium in a glass chamber, between two parallel surfaces made of a force transducer probe of borosilicate glass and the bottom surface of the chamber, as illustrated in figure 1. The force imposed on the cell is measured simultaneously by the force transducer. The details of the technique, including a schematic of the micromanipulation rig and video image of a single cell being compressed between the two surfaces, are described in Nguyen *et al.* (2009*b*). The precision of the force and displacement measurements is ±0.01 μN and ±0.2 μm, respectively (Thomas *et al.* 2000). Single spherical chondrocytes and chondrons with diameters of 8.7–9.3 and 9.3–9.9 μm, respectively, were compressed to a wide range of deformations at a given speed. The cells were held at a constant deformation to permit them to relax, and then released by lifting the probe to move backwards to its original position at the same speed as compression. During compression, holding and release, the force being imposed on the cells was measured. From these measurements, force–displacement and force–time data were obtained. In this paper, the behaviour of single chondrocytes and chondrons, compressed with a speed of 6 μm s^{-1} to a final nominal strain of 30 per cent, held for approximately 3 s, released at the same speed and then compressed to a final nominal strain of 50 per cent, held and released, was simulated by finite-element modelling. The terminology 'nominal strain' used in this paper context is defined as the ratio between the applied displacement in the direction of compression and the original cell diameter.

3. FINITE-ELEMENT MODELLING

3.1. Assumptions and finite-element model

A model of the compression–holding–release of a single cell was developed in Abaqus (ABAQUS 2005). The

cell was assumed to be incompressible, isotropic and homogeneous. Its initial shape was taken to be spherical, which is consistent with microscopic observations and images from the high-speed camera (Nguyen *et al.* 2009*b*). By taking advantage of axisymmetry and an equatorial plane of symmetry, only a quarter of the cross section was modelled, as shown in figure 1. Support nodes were defined to represent the symmetry conditions and to restrain fully the top plate as required for displacement loads. Supports on the left side of the quarter of cross section (figure 1) allowed movements in the direction of compression, and rotation, while supports at the bottom (90° to the direction of compression) allowed movements in the x-direction, and rotation.

The probe tip was modelled as a rigid flat surface since glass has a Young's modulus in the range of 62–76 GPa (Budinski 1979). The whole cell (chondrocyte or chondron) was modelled by 1615 axisymmetric solid elements. The contact between the compression probe and the cell was modelled as a surface-to-surface contact and was assumed to be frictionless. A mesh convergence study was performed to ensure that the mesh chosen was sufficiently accurate.

In the simulations, as in the experiments, the cell was compressed with a speed of 6 μm s^{-1} up to a final nominal strain of 30 per cent, held for approximately 3 s and then released to perform unloading; this process was then repeated for a final nominal strain of 50 per cent. As the compression deformation was large, any geometric and material nonlinearities that occurred within the model were taken into account, thereby effectively modelling large strains (as described later in §§ 3.2 and 3.3) and rotations. For the elastic material model, the *HYPERELASTIC procedure (ABAQUS 2005) was used, while for the viscoelastic material model, the *VISCO procedure (ABAQUS 2005) was used to determine the response of the cell to the applied displacement.

3.2. Nonlinear elastic material model

For the compression to 30 per cent final nominal strain, the cell was modelled as an incompressible, isotropic, homogeneous, neo-Hookean nonlinear elastic model throughout the test from loading and holding. The neo-Hookean strain energy takes the following form (Rivlin 1948):

$$U = C_{10}(\bar{I}_1 - 3) + \frac{1}{D_1}(J^{\mathrm{el}} - 1)^2, \tag{3.1}$$

where U is the strain energy per unit of undeformed volume; $\bar{I}_1 = \bar{\lambda}_1^2 + \bar{\lambda}_2^2 + \bar{\lambda}_3^2$ is the first deviatoric strain invariant defined through the deviatoric stretches $\bar{\lambda}_i = J^{-1/3}\lambda_i$ (where λ_i are the principal stretches and J is the total volume ratio); J^{el} is the elastic volume ratio; and C_{10} and D_1 are material parameters related to the shear modulus (G), elastic modulus (E) and bulk modulus (K) by $G = E/2(1+\upsilon) = 2C_{10}$ and $K = 2/D_1$, where υ is Poisson's ratio. For an incompressible material, $D_1 = 0$, $\upsilon = 0.5$ and $J = J^{\mathrm{el}} = 1$.

The constitutive equation can be expressed in the following form (Spencer 2009):

$$\boldsymbol{\sigma} = 2\frac{\partial U}{\partial \bar{I}_1}\mathbf{B} - p\mathbf{I}, \tag{3.2}$$

where $\boldsymbol{\sigma}$ is the Cauchy stress tensor, p is the hydrostatic pressure, $\mathbf{I}$ is the identity tensor, $\mathbf{B} = \mathbf{F}\mathbf{F}^{\mathbf{T}}$ is the Cauchy–Green deformation tensor, $\mathbf{F}$ is the deformation gradient tensor and the superscript T denotes the transpose.

3.3. Viscoelastic material model

A viscoelastic material model was used in the simulation of compression to a 50 per cent final nominal strain and then holding. It was also assumed that the cell was incompressible as in many prior studies (Trickey *et al.* 2000; Guilak *et al.* 2002; Koay *et al.* 2003; Leipzig & Athanasiou 2005; Ofek *et al.* 2009*a*).

For the compression of a 50 per cent final nominal strain, the cell was modelled in ABAQUS as a neo-Hookean nonlinear viscoelastic material. The stress–strain relationship of an incompressible, homogeneous, isotropic, nonlinear viscoelastic material is defined by a generalized Maxwell model and has a hereditary integral formulation:

$$\sigma_{ij}(t) = \int_0^t 2G(t-s)\dot{\gamma}_{ij}(s)\,\mathrm{d}s + \int_0^t K(t-s)\dot{\varepsilon}_{kk}^{\mathrm{vol}}(s)\delta_{ij}\,\mathrm{d}s, \tag{3.3}$$

where $\sigma_{ij}(t)$ is the ijth component of the stress tensor; $G(t)$ and $K(t)$ are the shear relaxation modulus and bulk relaxation modulus, respectively, which are functions of the time, t; $\gamma_{ij}(s)$ and $\varepsilon_{kk}^{\mathrm{vol}}(s)$ are the ijth and kkth components of deviatoric and volumetric strain tensors at reduced time s, respectively; $\dot{\gamma}_{ij}(s)$ and $\dot{\varepsilon}_{kk}^{\mathrm{vol}}(s)$ are the ijth and kkth components of the first derivative of the deviatoric and volumetric strain tensors at reduced time s, respectively; The double subscripts in $\dot{\varepsilon}_{kk}^{\mathrm{vol}}(s)$ adopt the summation convention. δ_{ij} is the Kronecker delta; $G(t)$ and $K(t)$ can be defined individually in terms of a series of exponentials known as the Prony series. For an incompressible material model, $K(t) = \infty$ and $\dot{\varepsilon}_{kk}^{\mathrm{vol}}(s) = 0$, leaving the right-hand side of equation (3.3) with only the first integral. In this paper, the Maxwell model reduced in this way was used, first with a 1-Prony series, and this is referred to as the three-parameter model. Equation (3.4*a*,*b*) gives the mathematical description of the model in shear relaxation form and load relaxation form (Nussinovitch *et al.* 1989; Andrei *et al.* 1996), and figure 2 shows its mechanical equivalents.

$$\frac{G(t)}{G_0} = \frac{G_\infty}{G_0} + \frac{G_1}{G_0}\mathrm{e}^{-t/\tau_1} \quad \text{with} \quad \frac{G_1}{G_0} + \frac{G_\infty}{G_0} = 1 \tag{3.4a}$$

and

$$\frac{F(t)}{F_0} = \frac{F_\infty}{F_0} + \frac{F_1}{F_0}\mathrm{e}^{-t/\tau_1} \tag{3.4b}.$$

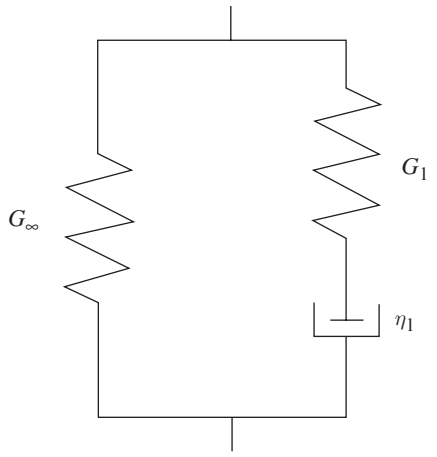

Figure 2. The generalized Maxwell model with three parameters.

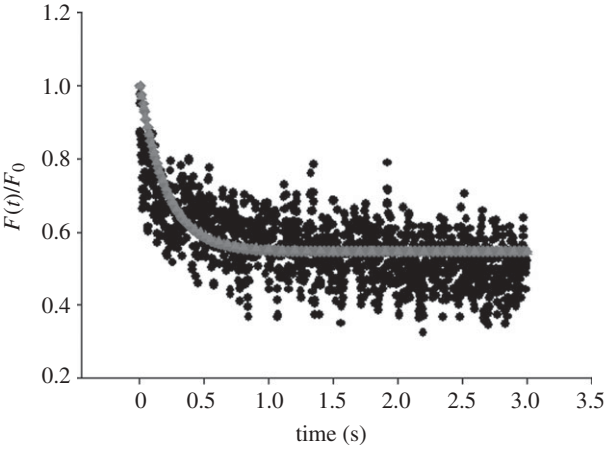

Figure 3. Experimental force relaxation data fitted by the load relaxation equation (3.4*b*) and the finite-element (FE) viscoelastic three-parameter model (regression coefficient for the fit, $r^2 = 0.99$). Filled circles, experiment; filled diamonds, fitting equation (3.4*b*); filled triangles, FE analysis.

In these equations, $G(t)$ is the shear relaxation modulus at time t; G_0 is the instantaneous shear modulus of the material; G_∞ is the shear modulus of the single spring and is called the long-term shear modulus or equilibrium shear modulus of the material; G_1 is the shear modulus of the spring in the Maxwell model; and τ_1 is the relaxation time ($\tau_1 = \eta_1/E_1$, where E_1 is Young's modulus of the spring, related to G_1 by $E_1 = 2(1+\upsilon)G_1$; and η_1 is the viscosity of the dashpot in the Maxwell model). The three parameters of equation (3.4*a*) are G_0, G_1 and τ_1. $F(t)$ in equation (3.4*b*) is the compressive force at time t; F_0 is the peak force at the end of the compression; F_∞ is the equilibrium force at the end of the relaxation; F_1 is the compressive force on the first component in the Maxwell model.

Finite-element modelling in Abaqus uses the shear relaxation form, but it is convenient to determine τ_1 directly from experimental force relaxation data using equation (3.4*b*), before determining the other parameters, i.e. the instantaneous shear modulus G_0 and G_1 or, equivalently, the normalized shear modulus $g_1 = G_1/G_0$. However, in this study, the instantaneous elastic modulus E_0 was used as a simulation parameter instead of G_0 because G_0 could be obtained from E_0 by the equation $G_0 = E_0/2(1+\upsilon) = E_0/3$ for an incompressible material.

3.4. Determination of the material parameters

For the elastic material model, fitting the finite-element simulations to the experimental data returned the material parameters. Two steps were used in determining the elastic modulus E. The first was determining the force at the end of compression F_0. Because there is no relaxation in an elastic model, F_0 was best determined as the average force from the experimental data in the holding phase. Then, the value of E could be found by adjusting its value so that the simulated value of F_0 matched the experimental value. The regression coefficient, r^2 (Gilbert 1981), was used to assess the quality of the fit between the simulation and experimental compression data.

For the viscoelastic material model, only the main steps are presented here as details can be found in Nguyen *et al.* (2009*b*).

- The load relaxation behaviour described by equation (3.4*b*) was fitted by the least-squares method to the normalized experimental force data from the relaxation phase to find values of F_1/F_0, F_∞/F_0 and the parameter τ_1. In this study, it was assumed that F_0 is the value of the peak force at the end of the compression phase, as used in Nguyen *et al.* (2009*a*,*b*). An example of the fitting is shown in figure 3.
- The shear relaxation equation (3.4*a*) was implemented in Abaqus for the relaxation phase only. The normalized force relaxation data from the finite-element modelling was fitted by the least-squares method to the normalized experimental data, using the relaxation time τ_1 found previously. An example of this is also shown in figure 3. From these fits, the parameters G_1/G_0 and G_∞/G_0 were found.
- It then remained to find G_0 or equivalently E_0. This could be done by adjusting the value of the latter until the finite-element simulations gave the correct value for F_0, i.e. the peak force at the end of the compression stage. Knowing G_0 and E_0 meant that the long-term elastic moduli E_∞ could also be calculated, see equation (3.4*a*). It should be noted that the apparent viscosity $\eta_1 = \tau_1 E_1$ is presented in this paper for comparison with previous studies.

By this fitting procedure, the best fit between simulated and experimental data in the relaxation phase was found, and the simulation gave the peak force correctly. Finally, the overall quality of fit was determined by determining the regression coefficient r^2 as described earlier.

3.5. Statistical analysis

The force–displacement and force–time data of 22 chondrocytes and 22 chondrons from Nguyen *et al.*

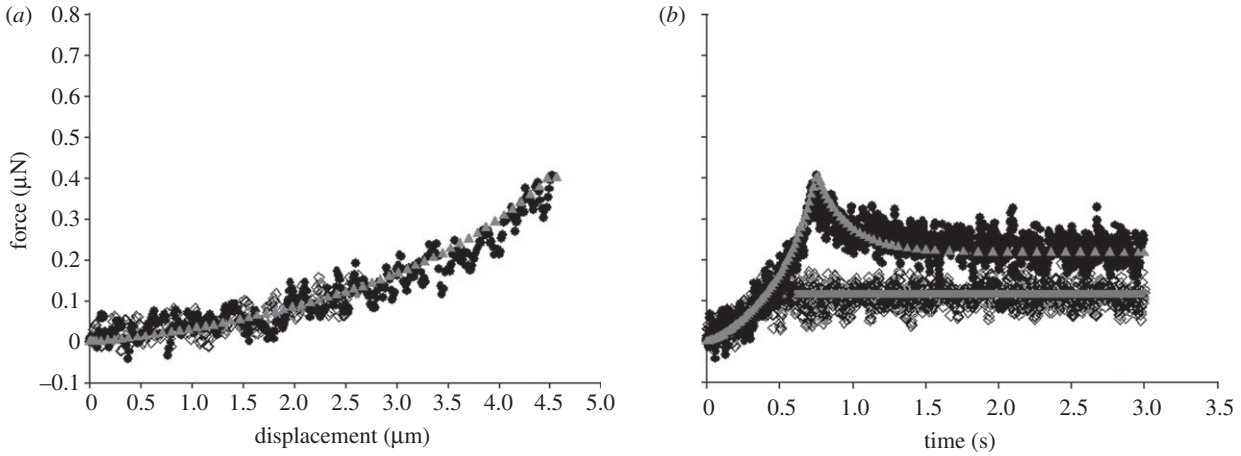

Figure 4. Typical (*a*) force–displacement curves and (*b*) force–time curves of a single chondrocyte compressed to 30 and 50% nominal strain, successively, and held. Compression speed of 6 $\mu m\,s^{-1}$. The diameter of the chondrocyte was 9.0 μm (regression coefficient for the fits of 30% nominal strain, $r^2 = 0.51$ in compression; regression coefficient for the fits of 50% nominal strain, $r^2 = 0.89$ in compression and $r^2 = 0.99$ in relaxation). FE, finite element. Open diamonds, experiment 30%; inverted triangles, FE analysis 30%; filled circles, experiment 50%; upright triangles, FE analysis 50%.

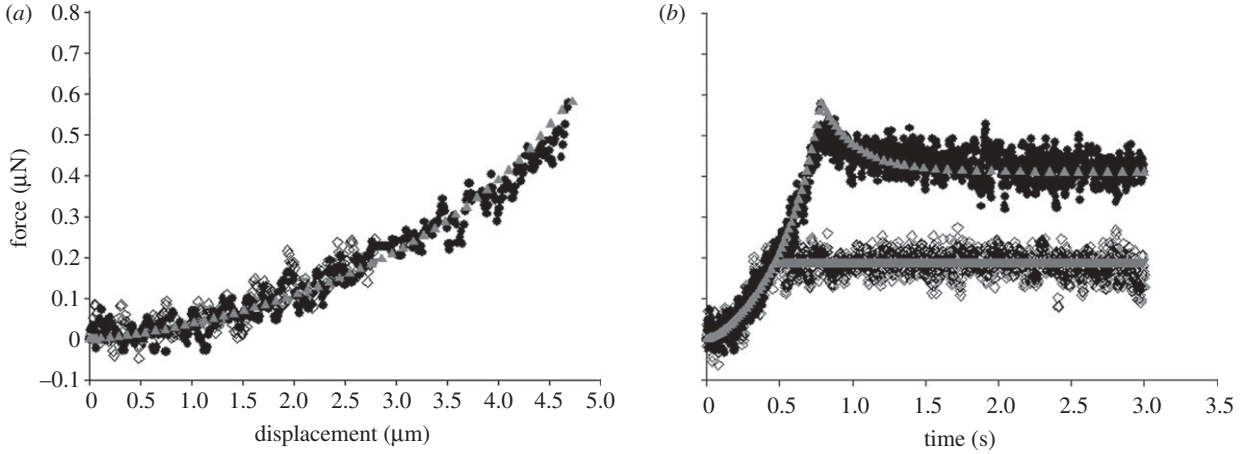

Figure 5. Typical (*a*) force–displacement curves and (*b*) force–time curves of a single chondron compressed to 30 and 50% nominal strain, successively, and held. Compression speed of 6 $\mu m\,s^{-1}$. The diameter of the chondron was 9.4 μm (regression coefficient for the fits of 30% nominal strain, $r^2 = 0.72$ in compression; regression coefficient for the fits of 50% nominal strain, $r^2 = 0.95$ in compression and $r^2 = 0.99$ in relaxation). Open diamonds, experiment 30%; inverted triangles, FE analysis 30%; filled circles, experiment 50%; upright triangles, FE analysis 50%.

(2009*b*) were assessed. Values of the mechanical property parameters of the cells were reported as mean ± standard error. Also, paired Student's *t*-tests were performed to determine whether significant differences existed between the mechanical properties of chondrocytes and chondrons, with statistical significance reported at the 95% confidence level ($p < 0.05$).

4. RESULTS

4.1. Elastic and viscoelastic behaviour

Figures 4 and 5 show typical force–displacement and force–time curves of a single chondrocyte (9.0 μm diameter) and chondron (9.4 μm diameter), respectively, compressed to nominal strains of 30 and 50 per cent, at a speed of 6 $\mu m\,ms^{-1}$ and then held for 3 s. The figures show that the larger the deformation at the end of compression, the greater the peak force on the cell and also the larger the subsequent force relaxation. When the final nominal strain was 30 per cent, the force relaxation was not significant, while there was considerable force relaxation at 50 per cent nominal strain. The force relaxation was attributed to viscoelasticity of the cells. After the force transducer had been moved back to its initial position, the cells fully recovered to their original shape, and there was no permanent deformation whether the final nominal strain was 30 or 50 per cent.

Table 1 presents the mechanical properties of the chondrocyte of figure 4 and the chondron of figure 5 from the modelling. In both cases, high values of the regression coefficient for the fits to the data with the final nominal strain of 50 per cent indicate an excellent agreement between the finite-element modelling and the experimental data. The relatively smaller values of the regression coefficient for the fits to the compression data with the final nominal strain of 30 per cent largely resulted from the noise at such force levels. For the nominal strain of 30 per cent, the elastic and viscoelastic

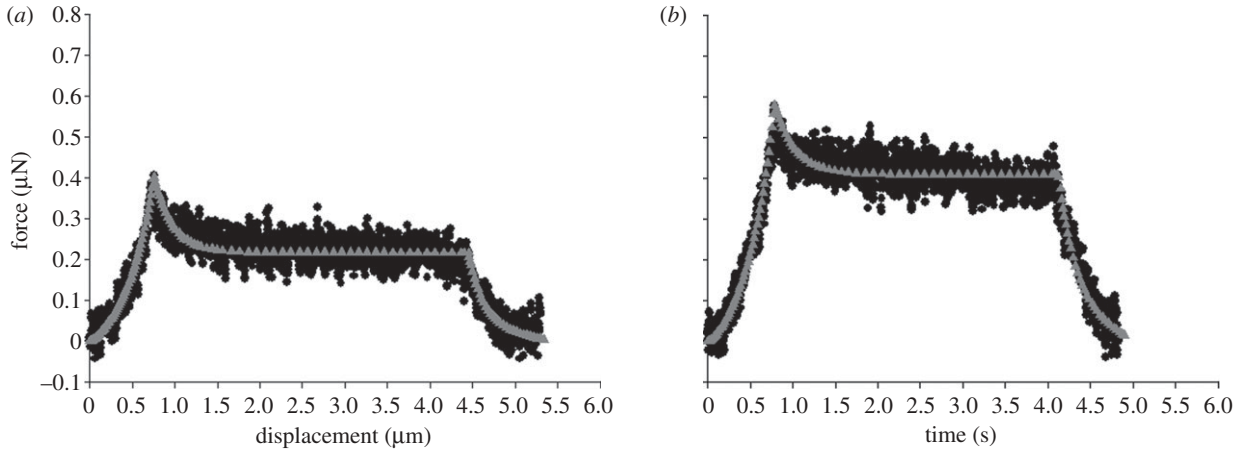

Figure 6. Typical force–time curves of (*a*) a single chondrocyte and (*b*) chondron compressed to 50% nominal strain, held and then released. Compression speed of 6 μm s^{-1}. The diameters of the chondrocyte and chondron were 9.0 and 9.4 μm, respectively. The regression coefficient for the unloading phase is $r^2 = 0.80$ and 0.93 for the chondrocyte and chondron, respectively. Filled circles, experiment 50%; filled triangles, FE analysis 50%.

Table 1. Mechanical properties of the chondrocyte of figure 4 and the chondron of figure 5 from elastic and viscoelastic models; final nominal strains of 30 and 50%, speed of 6 μm s^{-1}.

		chondrocyte		chondron	
material model	mechanical properties	30% deformation	50% deformation	30% deformation	50% deformation
elastic	E (kPa)	15	—	21	—
viscoelastic	E_0 (kPa)	—	24	—	29
	E_∞ (kPa)	—	7.7	—	13.6
	η_1 (kPa s)	—	3.4	—	3.1

models give force values of 0.12 and 0.13 μN, respectively, for the chondrocyte (figure 4*b*), and the force difference is insignificant. For the chondron as shown in figure 5*b*, the corresponding force values given by the two models are all 0.19 μN. The insignificant difference in the force value given by the two models demonstrates the consistency of the modelling work. It should be noted that the apparent viscosity $\eta_1 = \tau_1 E_1$ is presented in this paper for comparison with previous studies.

The material properties of the cells were then used for modelling of unloading of the cells after holding. Comparisons of the finite-element prediction and the experimental data are shown in figure 6. Excellent agreement with the experimental data further confirms the validity of the finite-element approach.

4.2. Material properties of cell populations

Twenty-two chondrocytes and 22 chondrons from Nguyen *et al.* (2009*b*) were selected for finite-element modelling to obtain population data. The chondrocytes had an average diameter of 9.0 ± 0.3 μm and chondrons had an average diameter of 9.6 ± 0.3 μm. These values compare well with previously published data (Leipzig & Athanasiou 2005; Darling *et al.* 2006; Shieh *et al.* 2006). The experimental data for each cell were fitted separately by the elastic and viscoelastic models to generate corresponding sets of mechanical property parameters. Good agreement between the finite-element modelling fits and the experimental data for both the elastic model (regression coefficient $r^2 \geq 0.56$) and the viscoelastic model were obtained ($r^2 \geq 0.70$ for compression and $r^2 \geq 0.98$ for relaxation). Table 2 presents the mechanical properties of chondrocytes and chondrons derived from the modelling.

Paired student's *t*-tests show a significant difference between the mean elastic moduli determined from 30 per cent nominal strain data and instantaneous moduli from 50 per cent nominal strain data for both chondrocytes and chondrons ($p < 0.05$); they also show a significant difference in the mean elastic and long-term moduli ($p < 0.04$), but no significant difference in the mean instantaneous moduli and viscosities ($p > 0.05$), between chondrocytes and chondrons.

5. DISCUSSION

Theoretically, it may be possible to fit the whole set of data (i.e. loading, compression and unloading) simultaneously using the least-square method to get unique values of E_0, E_∞ and η. However, it is extremely time consuming, if not impossible, to implement the approach since there are three unknown parameters that need to be optimized using the finite-element analysis. A step-by-step approach was chosen, fitting the force relaxation and compression separately. The fitting in each step was optimized and the resulting values of E_0, E_∞ and η were then used to predict the

Table 2. Mechanical properties of chondrocytes and chondrons ($n = 22$) from elastic and viscoelastic models; final nominal strains of 30 and 50%, speed of 6 $\mu m\,s^{-1}$. The fit in compression at 30% nominal strain of the elastic model returned $r^2 = 0.56 \pm 0.04$ and 0.61 ± 0.04 for chondrocytes and chondrons, respectively. The best fit in compression at 50% nominal strain of the viscoelastic model for relaxation data were $r^2 = 0.98$ and 0.99 for chondrocytes and chondrons, respectively; while for compression data, the fits returned $r^2 = 0.70 \pm 0.04$ and 0.72 ± 0.04 for chondrocytes and chondrons, respectively; the results are presented as mean $\pm$ s.e.

		chondrocytes ($n = 22$)		chondrons ($n = 22$)	
material model	mechanical properties	30% deformation	50% deformation	30% deformation	50% deformation
elastic	E (kPa)	14 ± 1	—	19 ± 2	—
viscoelastic	E_0 (kPa)	—	21 ± 3	—	27 ± 4
	E_∞ (kPa)	—	9.3 ± 0.8	—	12 ± 1
	η_1 (kPa s)	—	2.8 ± 0.5	—	3.4 ± 0.6

force versus displacement/time for unloading. The high value of the regression coefficient for each step justifies this step-by-step approach.

The results demonstrated that both chondrocytes and chondrons in suspension showed significantly viscoelastic behaviour when the nominal strain at the end of compression was 50 per cent, but were generally elastic at 30 per cent nominal strain or lower (Nguyen *et al.* 2009*b*). The good agreement of the models implies that the cells behaved as viscoelastic solids at 50 per cent nominal strain, while remaining elastic at 30 per cent nominal strain. Such strain-dependent viscoelastic behaviour of the cells has been observed in other studies using different loading devices (Wang *et al.* 1993; Wang & Ingber 1994; Shieh *et al.* 2006). The difference in cell behaviour at 30 and 50 per cent nominal strains might be due to the inhomogeneous structure of chondrocytes and chondrons, the mechanical behaviour of both of which was strain-dependent (Shieh *et al.* 2006; Nguyen *et al.* 2009*b*). At small deformation, the mechanical behaviour of chondrocytes may be governed primarily by their membrane, which may be considered to be largely elastic. For chondrons at small deformation, both the PCM and cell membrane may be responsible for their mechanical behaviour. As the deformation is increased, some other intracellular components such as the cytoskeleton and nucleus may play an increasingly significant role. It is known that the cytoskeleton and nucleus can show viscoelastic behaviour (Dong *et al.* 1991; Guilak *et al.* 2000; Trickey *et al.* 2004), and they may contribute increasingly to the whole-cell response as single cells are deformed further. Ofek *et al.* (2009*b*) have recently investigated the contribution of the main three cytoskeletal elements (actin microfilaments, intermediate filaments and microtubules) to the bulk compressive stiffness, volumetric or apparent compressibility changes and recovery behaviour of individual chondrocytes attached to a glass slide, and found that actin microfilaments were the largest contributor to bulk cell compressive stiffness and cell volume, intermediate filaments fettered transverse cell expansion while microtubules contributed to the incompressive nature of cells and maintained the critical strain threshold and time constant in cellular recovery behaviour. It may be hypothesized that when the nominal strain at the end of compression was 30 per cent or less, the elastic behaviour of the cell membrane dominated, while compression of the cytoskeleton and nucleus at 50 per cent nominal strain led to considerable viscoelasticity. In support of this hypothesis, comparison of the mechanical properties of cells (table 2 and §3.5) also revealed significant differences between the mean elastic and mean instantaneous moduli. This suggests that the cytoskeleton and cell nucleus are not only viscoelastic but are significantly stiffer than the membrane, which is consistent with the previous studies (Guilak *et al.* 2000; Knight *et al.* 2002; Trickey *et al.* 2004). It should be mentioned that the nucleus of a chondrocyte might also be deformed significantly at a whole-cell nominal strain of 30 per cent (Guilak 1995; Lee *et al.* 2000; Leipzig & Athanasiou 2008). However, the chondrocytes investigated by these researchers were either adherent or embedded in construct or cartilage tissue, and therefore might behave differently from the single cells in suspension of this work.

The data in table 2 show that chondrons had significantly greater mean elastic and mean long-term moduli than chondrocytes, with 95% confidence. The PCM appeared to substantially influence the mechanical properties of the cells. This is a plausible observation when compared with previous studies using micropipette aspiration (Alexopoulos *et al.* 2003, 2005; Guilak *et al.* 2005). These earlier studies showed that the PCM exhibited elastic behaviour and its elastic modulus had values in a large range 1.5–68.9 kPa, which is much higher than the elastic modulus of the whole chondrocyte, i.e. in the range 0.1–8 kPa (Trickey *et al.* 2000; Knight *et al.* 2002; Koay *et al.* 2003; Shieh & Athanasiou 2006). More direct comparisons are not possible as this study did not measure the PCM mechanical properties separately from the whole cell. So far, micropipette aspiration and AFM have been used to measure the mechanical properties of the PCM of single chondrons. The results of the present study have demonstrated the feasibility of compression testing of single chondrons at large deformations, which combined with additional finite-element modelling, e.g. modelling chondrons with a core/shell structure, should allow further investigations of the role of PCM in chondrons.

It should be noted that the results in table 2 do not show a significant difference in the mean instantaneous moduli and the mean viscosities between chondrocytes

Table 3. Comparison of the mechanical properties to previous elastic and viscoelastic modelling of single chondrocytes. These results presented as mean ± s.d.

model	mechanical properties	micro-manipulation	modified cytoindentation[a]	cytoindentation[b]	micropipette aspiration[c]	AFM[d,e]
elastic	E (kPa)	14 ± 1	2.55 ± 0.85	—	—	2.3–3
viscoelastic	E_0 (kPa)	21 ± 3	2.47 ± 0.85	8.0 ± 4.41	0.41 ± 0.17	0.29 ± 0.14
	E_∞ (kPa)	9.3 ± 0.8	1.48 ± 1.80	1.09 ± 0.40	0.24 ± 0.11	0.17 ± 0.09
	η_1 (kPa s)	2.8 ± 0.5	1.92 ± 1.80	1.50 ± 0.92	3.0 ± 1.80	0.61 ± 0.69

[a]Leipzig & Athanasiou (2005).
[b]Koay *et al.* (2003).
[c]Trickey *et al.* (2000).
[d]Ng *et al.* (2007).
[e]Darling *et al.* (2006).

and chondrons. A possible explanation for this is that these two parameters might be largely determined by the viscoelastic properties of the cell cytoskeleton and nucleus. If it is presumed that the cytoskeletons and nuclei of chondrocytes and chondrons have similar properties, the overall viscoelastic mechanical properties would not be very different. Even so, the other results (i.e. elastic modulus and long-term modulus) show that there is a significant difference in the mechanical properties between chondrocytes and chondrons.

Table 3 illustrates a comparison of elastic and viscoelastic material properties from this study and previous studies. Overall, the values of the mechanical property parameters of single chondrocytes obtained by the nonlinear elastic and viscoelastic models used in this study are in the same order of magnitude as those from previous studies (Trickey *et al.* 2000; Koay *et al.* 2003; Leipzig & Athanasiou 2005; Darling *et al.* 2006; Ng *et al.* 2007). However, in comparison to AFM and previous experiments, the data from micromanipulation compression yielded higher values of E_0 and E_∞. This could be attributed to several factors, most obviously the inhomogeneous structure of cells and differences in testing methodologies. Micromanipulation compressed the entire cell to a large nominal strain, i.e. 30 or 50 per cent, while AFM, micropipette and cytoindentation only deformed a portion of the cell's membrane. The modified cytoindentation method of Leipzig & Athanasiou (2005) compressed the cell up to 40 per cent nominal strain, but their data were only fitted with the assumption of small deformation. It is important to note that the cytoskeleton and nucleus might have noticeable effects on the cell's response during compression at large deformation by micromanipulation, whereas it probably had a significantly smaller contribution in other methods, especially AFM and micropipette aspiration. This is supported by previous studies using AFM, micropipette aspiration and micromanipulation techniques (Guilak *et al.* 2000; Mathur *et al.* 2000; Caille *et al.* 2002; Knight *et al.* 2002) which have shown that isolated nuclei from cells are 3–16 times stiffer than the cells. Moreover, though modified cytoindentation (Leipzig & Athanasiou 2005) might compress the entire cell, the mechanical properties of cells were still different from those obtained by micromanipulation. This could arise from the fact that micromanipulation was conducted on suspended cells (cells in culture medium), whereas modified cytoindentation tested cells adhered to a substratum. The cells in suspension were observed to be spherical, so were modelled as spheres in this study, and were idealized as homogeneous and isotropic. The model of modified cytoindentation of Leipzig & Athanasiou (2005) made the same assumption even though the cells were represented as ellipsoids, indicating that the cells under this condition had a non-isotropic structure.

Furthermore, the cells were assumed to be incompressible in this study, as it is not yet possible to measure the volume change in such small cells accurately in compression testing by micromanipulation. In prior studies, it was shown via hydrostatic pressurization that MG63 osteosarcoma cells were intrinsically incompressible (Wikes & Athanasiou 1996), suggesting that this assumption of cell incompressibility was reasonable. Also, supporting this assumption, no volume change has been observed experimentally in single chondrocytes subjected to compression at strain levels below 30–35% (Koay *et al.* 2008). However, in the recent study of Shieh & Athanasiou (2006) using the modified cytoindentation technique, it was found that chondrocytes exhibit substantial compressibility (i.e. Poisson's ratio of 0.18–0.34). It was then suggested that the resulting instantaneous modulus, long-term modulus and apparent viscosity of cells were 19 per cent higher than if cells were assumed to be incompressible. Therefore, further experiments will need to examine the compressibility of chondrocytes and chondrons using the micromanipulation technique.

Compression of single chondrocytes and chondrons was modelled to be elastic at a final nominal strain of 30 per cent and viscoelastic at 50 per cent. Chondrons have a layer of PCM that itself may be considered to be poroelastic (Lee *et al.* 2010) or poroviscoelastic. However, it is believed that the layer of PCM was very thin for the chondrons investigated here since their diameters (9.6 ± 0.3 μm) differed only marginally from those of chondrocytes (9.0 ± 0.3 μm). Therefore, a combination of the elastic and viscoelastic model for the whole chondrocyte and chondron was chosen rather than a poroelastic/poroviscoelastic model. Nevertheless, this work indicates the limitation of assuming chondrocytes and chondrons to be homogeneous in determination of their mechanical properties. Future

work should consider modelling the mechanical properties of individual intracellular components of chondrocytes and chondrons in order to understand better their strain-dependent mechanical behaviour.

It can be concluded that the micromanipulation technique and finite-element modelling with nonlinear elastic and viscoelastic material models can be used to identify biomechanical properties of single chondrocytes and chondrons. As the deformation generated by compression is increased, the mechanical response of cells may be more and more dominated by the cell cytoskeleton and/or nucleus rather than the membrane. Conventional techniques such as micropipette aspiration and AFM tend to give information about local mechanical properties such as cell membrane or PCM, while the data obtained using micromanipulation based on compression of single cells to large deformations between two infinite parallel surfaces also reflect the mechanical properties of other intracellular components such as the cytoskeleton and nucleus. The results are novel as there has been a paucity of information to date about such biomechanical properties of single chondrocytes and chondrons, especially from direct compression up to large deformations.

We acknowledge the Engineering and Physical Sciences Research Council (EP/C51127/1), UK, for sponsoring this work.

REFERENCES

ABAQUS 2005 *Analysis user's manual,* v. 6.5. Pawtucket, RI: Hibbit, Karlsson and Sorensen Inc.

Alexopoulos, L. G., Haider, M. A., Vail, T. P. & Guilak, F. 2003 Alterations in the mechanical properties of the human chondrocyte pericellular matrix with osteoarthritis. *J. Biomech. Eng.* (*Trans. ASME*) **125**, 323–333. (doi:10.1115/1.1579047)

Alexopoulos, L. G., Setton, L. A. & Guilak, F. 2005 The biomechanical role of the chondrocyte pericellular matrix in articular cartilage. *Acta Biomater.* **1**, 317–325. (doi:10.1016/j.actbio.2005.02.001)

Allen, D. M. & Mao, J. J. 2004 Heterogeneous nanostructural and nanoelastic properties of pericellular and interterritorial matrices of chondrocytes by atomic force microscopy. *J. Struct. Biol.* **145**, 196–204. (doi:10.1016/j.jsb.2003.10.003)

Andrei, D. C., Briscoe, B. J., Luckham, P. F. & Williams, D. R. 1996 The deformation of microscopic gel particles. *J. Chim. Phys. Phys. Chim. Biol.* **93**, 960–976.

Athanasiou, K. A., Thoma, B. S., Lanctot, D. R., Shin, D., Agrawal, C. M. & LeBaron, R. G. 1999 Development of the cytodetachment technique to quantify mechanical adhesiveness of the single cell. *Biomaterials* **20**, 2405–2415. (doi:10.1016/S0142-9612(99)00168-4)

Buckwalter, J. & Mankin, H. 1998 Articular cartilage: tissue design and chondrocyte–matrix interactions. *Instr. Course Lect.* **47**, 477–486.

Budinski, K. G. 1979 *Engineering materials: properties and selection.* Reston, VA: Reston Publishing Company, Inc.

Caille, N., Thoumine, O., Tardy, Y. & Meister, J. 2002 Contribution of the nucleus to the mechanical properties of endothelial cells. *J. Biomech.* **35**, 177–187. (doi:10.1016/S0021-9290(01)00201-9)

Darling, E. M., Zauscher, S. & Guilak, F. 2006 Viscoelastic properties of zonal articular chondrocytes measured by atomic force microscopy. *Osteoarthritic Cartilage* **14**, 571–579. (doi:10.1016/j.joca.2005.12.003)

Dong, C., Skalak, R. & Sung, L. P. 1991 Cytoplasmic rheology of passive neutrophils. *Biorheology* **28**, 557–567.

Gilbert, N. 1981 *Statistics*, pp. 328–340, 2nd edn. Japan: Saunders College Publishing.

Guilak, F. 1995 Compression-induced changes in the shape and volume of the chondrocyte nucleus. *J. Biomech.* **28**, 1529–1541. (doi:10.1016/0021-9290(95)00100-X)

Guilak, F. & Mow, V. C. 2000 The mechanical environment of the chondrocyte: a biphasic finite element model of cell–matrix interactions in articular cartilage. *J. Biomech.* **33**, 1663–1673. (doi:10.1016/S0021-9290(00)00105-6)

Guilak, F., Ratcliffe, A. & Mow, V. C. 1997 Physical regulation of cartilage metabolism. In *Basic orthopedic biomechanics* (eds W. C. Hayes & V. C. Mow), pp. 179–207. Philadelphia, PA: Lipincott-Ravenwood.

Guilak, F., Jones, W. R., Ting-Beall, H. P. & Lee, G. M. 1999 The deformation behavior and mechanical properties of chondrocytes in articular cartilage. *Osteoarthritis Cartilage* **7**, 59–70. (doi:10.1053/joca.1998.0162)

Guilak, F., Tedrowa, J. R. & Burgkartb, R. 2000 Viscoelastic properties of the cell nucleus. *Biochem. Biophys. Res. Commun.* **269**, 781–786. (doi:10.1006/bbrc.2000.2360)

Guilak, F., Erickson, G. R. & Ting-Beall, H. P. 2002 The effects of osmotic stress on the viscoelastic and physical properties of articular chondrocytes. *Biophys. J.* **82**, 720–727. (doi:10.1016/S0006-3495(02)75434-9)

Guilak, F., Alexopoulos, L. G., Haider, M. A., Ting-Beall, H. P. & Setton, L. A. 2005 Zonal uniformity in mechanical properties of the chondrocyte pericellular matrix: micropipette aspiration of canine chondrons isolated by cartilage homogenization. *Ann. Biomed. Eng.* **33**, 1312–1318. (doi:10.1007/s10439-005-4479-7)

Knight, M. M., van de Breevaart Bravenboer, J., Lee, D. A., van Osh, G. J. V. M., Weinans, H. & Bader, D. L. 2002 Cell and nucleus deformation in compressed chondrocyte–alginate constructs: temporal changes and calculation of cell modulus. *Biochim. Biophys. Acta* **1570**, 1–8.

Koay, E. J., Shieh, A. C. & Athanasiou, K. A. 2003 Creep indentation of single cells. *J. Biomech. Eng.* **125**, 334–341. (doi:10.1115/1.1572517)

Koay, E. J., Ofek, G. & Athanasiou, K. A. 2008 Effects of TGF-β1 and IGF-I on the compressibility, biomechanics, and strain-dependent recovery behavior of single chondrocytes. *J. Biomech.* **41**, 1044–1052. (doi:10.1016/j.jbiomech.2007.12.006)

Kuettner, K. E., Pauli, B. U., Gallm, G., Memoli, V. A. & Schenk, R. K. 1982 Synthesis of cartilage matrix by mammalian chondrocytes *in vitro*. I. Isolation, culture characteristics, and morphology. *J. Cell Biol.* **93**, 743–750. (doi:10.1083/jcb.93.3.743)

Lee, G. M., Poole, C. A., Kelley, S. S., Chang, J. & Caterson, B. 1997 Isolated chondrons: a viable alternative for studies of chondrocyte metabolism *in vitro*. *Osteoarthritis Cartilage* **5**, 261–274. (doi:10.1016/S1063-4584(97)80022-2)

Lee, D. A., Knight, M. M., Bolton, J. F., Idowu, B. D., Kayser, M. V. & Bader, M. 2000 Chondrocyte deformation within compressed agarose constructs at the cellular and subcellular levels. *J. Biomech.* **33**, 81–95. (doi:10.1016/S0021-9290(99)00160-8)

Lee, B., Han, L., Frank, E. H., Chubinskaya, S., Ortiz, C. & Grodzinsky, A. J. 2010 Dynamic mechanical properties of the tissue-engineered matrix associated with individual chondrocytes. *J. Biomech.* **43**, 469–476. (doi:10.1016/j.jbiomech.2009.09.053)

Leipzig, N. D. & Athanasiou, K. A. 2005 Unconfined creep compression of chondrocytes. *J. Biomech.* **38**, 77–85.

Leipzig, N. D. & Athanasiou, K. A. 2008 Static compression of single chondrocytes catabolically modifies single-cell gene expression. *Biophys. J.* **94**, 2412–2422. (doi:10.1529/biophysj.107.114207)

Mathur, A. B., Truskey, G. A. & Reichert, W. M. 2000 Atomic force and total internal reflection fluorescence microscopy for the study of force transmission in endothelial cells. *Biophys. J.* **78**, 1725–1735. (doi:10.1016/S0006-3495(00)76724-5)

Ng, L., Hung, H.-H., Sprunt, A., Chubinskaya, S., Ortiz, C. & Grodzinsky, A. 2007 Nanomechanical properties of individual chondrocytes and their developing growth factor-stimulated pericellular matrix. *J. Biomech.* **40**, 1011–1023. (doi:10.1016/j.jbiomech.2006.04.004)

Nguyen, V. B., Wang, C. X., Thomas, C. R. & Zhang, Z. 2009*a* Mechanical properties of single alginate microspheres determined by microcompression and finite element modelling. *Chem. Eng. Sci.* **64**, 821–829. (doi:10.1016/j.ces.2008.10.050)

Nguyen, V. B., Wang, Q. G., Kuiper, N. J., El Haj, A. J., Thomas, C. R. & Zhang, Z. 2009*b* Strain-dependent viscoelastic behaviour and rupture force of single chondrocytes and chondrons under compression. *Biotechnol. Lett.* **31**, 803–809. (doi:10.1007/s10529-009-9939-y)

Nussinovitch, A., Pleg, M. & Normand, M. D. 1989 A modified Maxwell and a nonexponential model for characterization of the stress relaxation of agar and alginate gels. *J. Food Sci.* **54**, 1013–1016. (doi:10.1111/j.1365-2621.1989.tb07934.x)

Ofek, G. & Athanasiou, K. A. 2007 Micromechanical properties of chondrocytes and chondrons: relevance to articular cartilage tissue engineering. *J. Mech. Mater. Struct.* **2**, 1059–1086. (doi:10.2140/jomms.2007.2.1059)

Ofek, G., Natoli, R. M. & Athanasiou, K. 2009*a* *In situ* mechanical properties of the chondrocyte cytoplasm and nucleus. *J. Biomech.* **42**, 873–877. (doi:10.1016/j.jbiomech.2009.01.024)

Ofek, G., Wiltz, D. C. & Athanasiou, K. 2009*b* Contribution of the cytoskeleton to the compressive properties and recovery behavior of single cells. *Biophys. J.* **97**, 1873–1882. (doi:10.1016/j.bpj.2009.07.050)

Peeters, E. A. G., Oomens, C. W. J., Bouten, C. V. C., Bader, D. L. & Baaijens, F. P. T. 2005 Mechanical and failure properties of single attached cells under compression. *J. Biomech.* **38**, 1685–1693. (doi:10.1016/j.jbiomech.2004.07.018)

Poole, C. A. 1997 Articular cartilage chondrons: form, function, and failure. *J. Anat.* **191**, 1–13. (doi:10.1046/j.1469-7580.1997.19110001.x)

Poole, C. A., Flint, M. H. & Beaumont, B. W. 1988 Chondrons extracted from canine tibial cartilage: preliminary report on their isolation and structure. *J. Orthop. Res.* **6**, 408–419. (doi:10.1002/jor.1100060312)

Rivlin, R. S. 1948 Large elastic deformations of isotropic materials. IV. Further development of the general theory. *Phil. Trans. R. Soc. Lond. A* **241**, 379–397.

Shieh, A. C. & Athanasiou, K. A. 2006 Biomechanics of single zonal chondrocytes. *J. Biomech.* **39**, 1595–1602. (doi:10.1016/j.jbiomech.2005.05.002)

Shieh, A. C., Koay, E. J. & Athanasiou, K. A. 2006 Strain-dependent recovery behavior of single chondrocytes. *Biomech. Model Mechanobiol.* **5**, 172–179. (doi:10.1007/s10237-006-0028-z)

Spencer, A. J. M. 2009 Ronald Rivlin and invariant theory. *Int. J. Eng. Sci.* **47**, 1066–1078. (doi:10.1016/j.ijengsci.2009.01.004)

Szirmai, J. A. 1974 The concept of the chondron as a biomechanical unit. In *Biopolymer und Biomechanik von Bindegewebssystemen* (ed. F. Hartmann), pp. 87–91. Berlin, Germany: Academic Press.

Thomas, C. R., Zhang, Z. & Cowen, C. 2000 Micromanipulation measurements of biological materials. *Biotechnol. Lett.* **22**, 531–537. (doi:10.1023/A:1005644412588)

Trickey, W. R., Lee, G. M. & Guilak, F. 2000 Viscoelastic properties of chondrocytes from normal and osteoarthritic human cartilage. *J. Orthop. Res.* **18**, 891–898. (doi:10.1002/jor.1100180607)

Trickey, W. R., Vail, T. P. & Guilak, F. 2004 The role of the cytoskeleton in the viscoelastic properties of human articular chondrocytes. *J. Orthop. Res.* **22**, 131–139. (doi:10.1016/S0736-0266(03)0150-5)

Wang, N. & Ingber, D. E. 1994 Control of cytoskeletal mechanics by extracellular matrix, cell shape, and mechanical tension. *Biophys. J.* **66**, 2181–2189. (doi:10.1016/S0006-3495(94)81014-8)

Wang, N., Butler, J. P. & Ingber, D. E. 1993 Mechanotransduction across the cell surface and through the cytoskeleton. *Science* **260**, 1124–1127. (doi:10.1126/science.7684161)

Wang, Q. G., El Haj, A. J. & Kuiper, N. J. 2008 Glycosaminoglycans in the pericellular matrix of chondrons and chondrocytes. *J. Anat.* **213**, 266–273. (doi:10.1111/j.1469-7580.2008.00942.x)

Wang, Q. G., Magnay, J. L., Nguyen, V. B., Thomas, C. R., Zhang, Z., El Haj, A. J. & Kuiper, N. J. 2009 Gene expression profiles of dynamically compressed single chondrocytes and chondrons. *Biochem. Biophys. Res. Commun.* **379**, 738–742. (doi:10.1016/j.bbrc.2008.12.111)

Wang, Q. G., Nguyen, B., Thomas, C. R., Zhang, Z., El Haj, A. J. & Kuiper, N. J. 2010 Molecular profiling of single cells in response to mechanical force: comparison of chondrocytes, chondrons and encapsulated chondrocytes. *Biomaterials* **31**, 1619–1625. (doi:10.1016/j.biomaterials.2009.11.021)

Wikes, R. P. & Athanasiou, K. A. 1996 The intrinsic incompressibility of osteoblast-like cells. *Tissue Eng.* **2**, 167–181.

Wong, M. & Carter, D. R. 2003 Articular cartilage functional histomorphology and mechanobiology: a research perspective. *Bone* **33**, 1–13. (doi:10.1016/S8756-3282(03)00083-8)